Original Research

BOLD MRI of Human Tumor Oxygenation During Carbogen Breathing

N. Jane Taylor, PhD,[1]* Hiram Baddeley, FRCR, FRACR,[1]
Kate A. Goodchild, MBBS, MRCP,[2] Melanie E. B. Powell, MD, FRCR,[2]
Michelle Thoumine, DCR,[1] Linda A. Culver, DCR,[1] J. James Stirling, DCR,[1]
Michele I. Saunders, MD, FRCR,[2] Peter J. Hoskin, MD, FRCR,[2] Heather Phillips, RGN,[2]
Anwar R. Padhani, MRCP, FRCR,[1] and John R. Griffiths, MBBS, DPhil,[3]

An MRI method is described for demonstrating improved oxygenation of human tumors and normal tissues during carbogen inhalation (95% O_2, 5% CO_2). T_2^*-weighted gradient-echo imaging was performed before, during, and after carbogen breathing in 47 tumor patients and 13 male volunteers. Analysis of artifacts and signal intensity was performed. Thirty-six successful tumor examinations were obtained. Twenty showed significant whole-tumor signal increases (mean 21.0%, range 6.5–82.4%), and one decreased (−26.5 ± 8.0%). Patterns of signal change were heterogeneous in responding tumors. Five of 13 normal prostate glands (four volunteers and nine patients with nonprostatic tumors) showed significant enhancement (mean 11.4%, range 8.4–14.0%). An increase in brain signal was seen in 11 of 13 assessable patients (mean 8.0 ± 3.7%, range 5.0–11.7%). T_2^*-weighted tumor MRI during carbogen breathing is possible in humans. High failure rates occurred due to respiratory distress. Significant enhancement was seen in 56%, suggesting improved tissue oxygenation and blood flow, which could identify these patients as more likely to benefit from carbogen radiosensitization. J. Magn. Reson. Imaging 2001;14:156–163. © 2001 Wiley-Liss, Inc.

Index terms: magnetic resonance imaging; carbogen; tumors; hypoxia

THE STUDY OF CEREBRAL BLOOD OXYGENATION by functional MRI (1) has led to noninvasive studies of blood supply and oxygenation in extracranial human tissues. These have now been extended to the study of tumors (2,3). The oxygenation status of cancer cells was shown by Gray et al (4) in 1953 to affect the outcome of radiotherapy, with more oxygenated cells being more radiosensitive. Since then, considerable research has been carried out on techniques that aim to increase radiosensitivity (5) with the aim of improving the efficacy of radiation treatment. Increasing the oxygen available to the cells can be accomplished by inhaling 100% oxygen (6), hyperbaric oxygen (7,8) and other high-oxygen gas mixtures such as carbogen (conventionally 95% O_2 and 5% CO_2) (6,9–13). Radiosensitizing agents such as nicotinamide (5,10) have also been investigated for their ability to improve the results of radiotherapy. A meta-analysis of radiosensitizer trials has shown significant improvements in both local control and survival in some, but not all tumors (14). The identification of patients who might benefit from the radiosensitizers is a difficult task, as the hypoxic fraction inside tumors needs to be assessed. T_2^*-weighted MR techniques show promise in being able to identify such regions within tumors noninvasively.

The image parameters in gradient-echo (GE) MR sequences may be manipulated to be sensitive to the deoxyhemoglobin (Hb) levels within red blood cells. Normally, blood contains a mixture of Hb and oxyhemoglobin (HbO). Hb is paramagnetic and HbO is diamagnetic, so deoxygenated blood appears darker on T_2^*-weighted images compared with oxygenated blood. Any increase in hemoglobin oxygen saturation would therefore be expected to cause an increase in the signal. The contrast is said to be blood oxygenation level dependent (BOLD) (1,15). Breathing high concentrations of oxygen should increase blood oxygen saturation and the measured signal from tissues on T_2^*-weighted images; however, the inhalation of 100% oxygen can cause a degree of vasoconstriction within tumor vessels. The addition of the vasodilator gas carbon dioxide to the oxygen (forming carbogen) is intended to counter this vasocon-

[1]Paul Strickland Scanner Centre, Mount Vernon Hospital, Northwood, Middlesex, United Kingdom.
[2]Marie Curie Research Wing for Oncology, Mount Vernon Hospital, Northwood, Middlesex, United Kingdom.
[3]CRC Biomedical MR Research Group, St George's Hospital, London United Kingdom.

Parts of this work were presented at the 4th Annual Meeting of ISMRM, New York, 1996 (Abstract 1313), and a preliminary report was published in Int J Radiat Oncol Biol Phys.

M.E.B. Powell is now at St. Bartholomew's Hospital, London United Kingdom.

Contract grant sponsors: Paul Strickland Cancer Centre; Charles Wolfson Charitable Trust; Contract grant sponsor: Cancer Research Campaign; Contract grant number: SP1989/0203.

*Address reprint requests to: J. T., Paul Strickland Scanner Centre, Mount Vernon Hospital, Northwood, Middlesex HA6 2RN, London, United Kingdom. E-mail: taylor@graylab.ac.uk

Received March 1, 2000; Accepted January 29, 2001.

striction. An additional effect of adding carbon dioxide to oxygen is to shift the HbO dissociation curve to the right (6). Compared with air, both the increased percentage of oxygen in the carbogen and the shift in the HbO curve will make more oxygen available in the capillaries and tend to increase the T_2^*-weighted image signal intensity. The increase in the acquired signal could also result from increased perfusion of magnetically unsaturated blood into the tumor (16,17). Large increases in signal have been observed with carbogen breathing in T_2^*-weighted GE MR images of transplanted tumors in animals. Such effects have been attributed to both perfusion and oxygenation changes (17–20). Imaging human tumors before and during the administration of a radiosensitizer and vasodilator such as carbogen may permit identification of regions with oxygenation and flow changes, which may in turn indicate regions of reversible hypoxia. Signal increases during carbogen breathing can also be expected in well vascularized normal tissues or at sites of physiological angiogenesis such as the premenopausal endometrium, the ovary, and benign prostatic hyperplasia. MRI measurements of changes induced by a carbon dioxide/air mixture in normal human brain have already been described by Rostrup et al (21).

In this work we describe our experience of T_2^*-weighted GE imaging in a variety of human tumors and normal tissues (prostate gland and brain). The effects of carbogen on the measured signal are described. The aim is to illustrate the technique utilized, examine the causes of failed examinations, and show the magnitude of the MR signal intensity changes observed with carbogen breathing.

METHODS

Patient Selection

A prospective clinical study of 47 patients and 13 male volunteers was performed. The study examinations were performed between March 1995 and June 1997. Our institution's committee on clinical research and medical ethics approved the study. Informed written consent was obtained. All studies were performed at the Paul Strickland Scanner Centre at Mount Vernon Hospital, London, U.K.

The median age of the patients was 63 years (range: 41–81 years) and of the male volunteers 34 years (range: 27–72 years). Patients were selected from those attending clinics at the hospital who were clinically well enough to undergo the MR examinations, and had not received any prior treatment. All histological groups were considered, but lesions had to be over 2 cm in size for inclusion. Tumors in the thorax and abdomen were excluded in most cases because respiratory, cardiac, and vessel pulsation motion in those regions resulted in severe MRI artifacts. The distribution of cases according to histological type and anatomical site is given in Table 1a and b. There were 14 patients with squamous cell carcinomas from primary tumors of the aerodigestive tract and nine adenocarcinomas arising from the rectum (five patients), prostate (three patients) and breast. Six patients had lymphomas, 10 patients had transitional carcinomas, and other histologies were present in eight patients.

MRI Protocols

Measurements were made using an Elscint Gyrex 2T-DLX MRI scanner (Haifa, India), running at 1.9T. Patients were positioned supine in the body coil with an anesthetic face mask comfortably but securely strapped in place. The patients' blood oxygen saturation and pulse rates were continually monitored by a pulse oximeter attached to a finger, and the respiration rate was recorded every minute by a radiographer, nurse, or anesthetist present in the magnet room.

Scout images of the tumor were acquired using a standard steady-state free precession (SSFP) sequence (TE = 11 ms, TR = 200 ms, flip angle = 90°, slice width = 10 mm, acquisition matrix = 200 (frequency encoding) by 256 (phase encoding), and zero-filled postreconstruction to 256^2 for display). The subjects were then brought out of the magnet and the mask was attached to a customized anesthetic circuit (22) and air cylinders. The gas flow rate was adjusted to be comfortable to the patient, and they were returned to the magnet. Details of the gas administration are given below. A second scout image was acquired to check slice position, and up to 30 sequential single-slice images were acquired at a single slice location using the same SSFP sequence with parameters TE = 60 ms, TR = 200 ms, flip angle = 40°, and other parameters identical to the scout (2,3). A delay was introduced between acquisitions, calculated to keep the time resolution to one image per minute.

Gas Inhalation Protocols

The success of the examinations depended on several factors, both psychological and physical. The most important was the breathing circuit design. We found that this should be capable of providing a flow rate of at least 20 liter/min^{-1}; most patients only needed 10–15 liter/min^{-1}, but a large lung capacity and hyperventilation in some patients caused the 3-liter bag to be insufficient at lower flow rates. The gas flow was continually modified by trained personnel throughout the examination to ensure it was sufficient. The mask should have valved inflow/outflow holes to prevent rebreathing, and to make breathing in and out equally comfortable.

A careful and complete explanation of what to expect was made to each patient and volunteer, so the hyperventilation did not panic them. Before the MRI examination, an evaluation for mask tolerance and carbogen tolerance was undertaken, by practicing with the circuit. Those unable to cope with either were not asked to proceed further. Intolerance did increase slightly when the masks were more tightly fitted. It was found that having another person inside the magnet room during the MRI procedures helped considerably, especially if they maintained physical contact with the patient.

As the effects of breathing carbogen are at a maximum after 5–10 minutes (23); the initial imaging protocol acquired images during 5 minutes of air breathing, 5 minutes of carbogen, and 5 minutes of air, with a

Table 1a
Summary of Technically Successful Examinations in 36 Patients

Tumor type	Ages (yrs)	Imaging site	Mean signal change (%)	Mean grey matter signal change (%)
Squamous carcinoma	59	Rectum	NSR	–
Squamous carcinoma	53	Neck nodes, primary	NSR	8.6 ± 8.6 $P = 0.047$
Squamous carcinoma	62	Larynx	NSR	7.9 ± 0.4 $P < 0.001$
Squamous carcinoma	66	Neck nodes	18.0 ± 16.5 $P = 0.007$	7.9 ± 4.3 $P < 0.001$
Squamous carcinoma	41	Neck nodes	29.9 ± 16.1 $P = 0.003$	5.4 ± 3.8 $P = 0.004$
Squamous carcinoma	68	Neck nodes	12.4 ± 7.6 $P = 0.001$	7.0 ± 4.4 $P < 0.001$
Squamous carcinoma+	75	Neck nodes	82.4 ± 16.1 $P < 0.001$	9.8 ± 2.3 $P = 0.012$
Squamous carcinoma	65	Neck nodes	21.8 ± 9.4 $P < 0.001$	7.1 ± 3.4 $P < 0.001$
Squamous carcinoma	49	Cheek	9.1 ± 5.6 $P = 0.001$	9.5 ± 7.4 $P = 0.01$
Lymphoma (NHL)	63	Sacrum	NSR	–
Lymphoma (NHL)	62	Neck nodes	NSR	5.0 ± 0.1 $P = 0.003$
Lymphoma (NHL)	76	Neck nodes	16.0 ± 12.6 $P = 0.01$	8.3 ± 0.2 $P < 0.001$
Lymphoma (NHL)	72	Neck nodes	16.4 ± 8.0 $P < 0.001$	NSR
Transitional carcinoma	76	Bladder	NSR	–
Transitional carcinoma	66	Bladder	NSR	–
Transitional carcinoma	61	Bladder	NSR	–
Transitional carcinoma	41	Bladder	10.3 ± 3.4 $P < 0.001$	–
Transitional carcinoma	51	Bladder	9.3 ± 2.8 $P < 0.001$	–
Transitional carcinoma	71	Bladder	9.3 ± 4.8 $P = 0.001$	–
Transitional carcinoma	72	Bladder	10.0 ± 4.5 $P < 0.001$	–
Transitional carcinoma	62	Bladder	36.3 ± 6.2 $P < 0.001$	–
Adenocarcinoma	76	Rectum	NSR	–
Adenocarcinoma	77	Rectum	NSR	–
Adenocarcinoma	58	Rectum	NSR	–
Adenocarcinoma	63	Rectum	NSR	–
Adenocarcinoma	61	Rectum	23.4 ± 9.9 $P < 0.001$	–
Adenocarcinoma	70	Prostate	NSR	–
Adenocarcinoma	66	Prostate	18.5 ± 8.6 $P < 0.001$	–
Adenocarcinoma	63	Prostate	11.0 ± 3.1 $P < 0.001$	–
Adenocarcinoma*	47	Breast	62.0 ± 23.4 $P = 0.004$	–
Cystic carcinoma*	57	Maxilliary Antrum	−26.5 ± 8.0 $P < 0.001$	11.7 ± 9.1 $P = 0.011$
Carcinoma ovary metastasis	56	Pelvis	NSR	–
Leiomyosarcoma	70	Prostate	9.8 ± 7.0 $P = 0.005$	–
Melanoma metastasis	61	Buttock	8.1 ± 6.5 $P = 0.013$	–
Osteosarcoma	74	Sacrum	6.5 ± 4.6 $P = 0.002$	–
Neuroblastoma	48	Nasal cavity	NSR	NSR

Statistically significant responses are given with ± 2 standard errors. In the responding tumors the mean signal change is over a region of interest of maximal response.
+Patient corresponds with data shown in Figures 1 and 2.
*Patients showed decreases in regional signal.
– = not applicable; NSR = no detectable or significant ($P > 0.05$) response.

Table 1b
Summary of Technical Failures in 11 Patients and 4 Volunteers

Tumour type	Age (yrs)	Imaging site	Cause of failure
Lymphoma (NHL)	81	Parotid	Movement
Lymphoma (NHL)	81	Maxilliary antrum	Movement
Transitional carcinoma	48	Bladder	Circuit intolerance
Transitional carcinoma	73	Bladder	Carbogen intolerance
Squamous carcinoma	76	Parotid	Movement
Squamous carcinoma	61	Tonsils	Movement
Squamous carcinoma	63	Larynx	Movement
Squamous carcinoma	75	Larynx	Movement
Squamous carcinoma	67	Piriform fossa	Movement
Angiosarcoma	41	Bronchus	Carbogen intolerance
Non-small cell carcinoma unknown primary	58	Neck nodes	Movement
None at exam site	29	Normal prostate	Susceptibility artefacts
None at exam site	34	Normal prostate	Susceptibility artefacts
None	27	Normal prostate	Susceptibility artefacts and claustrophobia
None	34	Normal prostate	Susceptibility artefacts and claustrophobia

5-minute transition period without imaging between them. This protocol evolved into continuous imaging for 30 minutes: 10 minutes air, 10 minutes carbogen, and a further 10 minutes of air. The final protocol was 5 minutes air, 10 minutes carbogen, and 10 minutes air, as it was found that the initial baseline air signal intensity was usually stable and the subject's tolerance of the procedure was improved by spending less time in the magnet with the mask in place.

Image Analysis

Fifteen images were used for analysis; the five which were acquired during the initial period of air breathing, the second five aquired during carbogen breathing, and the second five acquired during the second period of air breathing, thus avoiding the five-minute transition periods. Images were transferred to a Sun Sparc10 (Sun Microsystems, Mountain View, CA) and converted to a raster-based format. They were analyzed using Analyze™ software (Mayo Foundation, Rochester, MN). Regions of interest (ROIs) were drawn from the T_1-weighted scout image, around the visible limits of the tumor. Color overlays were used to help identify regions that increased significantly in signal intensity with the carbogen breathing. Statistical analysis was performed using analysis of variance of the mean ± SD of the 15-image ROI data sets, and professional statistical advice was sought in these evaluations. Final results are given as mean response ± 2 standard error, where 1 standard error = SD of the mean/$\sqrt{}$ number of pixels in the ROI.

RESULTS

General

Of the first 37 patients imaged, there was a rise in pulse rate in seven, a decrease in 17, and no change in 13. The respiration rate increased in 25, decreased in two, and remained static in 10. There was no correlation between the T_2^*-weighted MRI signal intensity response of the tumors and the pulse or respiration rates. MRI results from tumor patients are given in Table 1a, a summary of failed examinations is given in Table 1b, and the results of the volunteer prostate studies are given in Table 2.

Tumor Patients

Eleven tumor measurements were technically invalid due to voluntary movement, mask displacement, intolerance of carbogen leading to panic and hyperventilation, or susceptibility artifacts (from air in the rectum in pelvis-tumor patients) (Table 1b). The mean GE MRI signal over the entire tumor ROI increased significantly ($P < 0.05$) during the carbogen breathing in 20 of the 36 successful tumor measurements (Table 1a). The range of significant enhancement was 6.5 ± 4.6% to 82.4 ± 16.1%, with a mean of 21.0%. Fifteen measurements showed no significant change with carbogen, and one decreased significantly (−26.5 ± 8.0%).

Enhancement was very heterogeneous: localized ROI within a tumor showed markedly different enhancement, and in two tumors there were areas of reduced signal surrounding central regions of enhancement during carbogen breathing. In two patients, in whom separate metastatic nodes were imaged simultaneously, one node enhanced whereas the other did not.

Figure 1 shows scout, subtraction, and air/carbogen BOLD images for a patient with a squamous carcinoma of the tongue and nodal metastases in the neck. This patient is indicated in Table 1a by * and the tumor positions by the arrows. The air and carbogen images are mean images, calculated by summing the five equilibrium images acquired with each gas, and dividing by 5. The first 5 minutes after a gas change was regarded as a transition period; the enhancement was calculated from the second 5-minute period in each case.

Figure 2 shows all the data from the larger node of patient *. There is a peak enhancement of 125.2% for the carbogen above the mean of the air values, although the mean enhancement over the entire node was 82.4% above the air value. The transition points are shown in the figure as triangles.

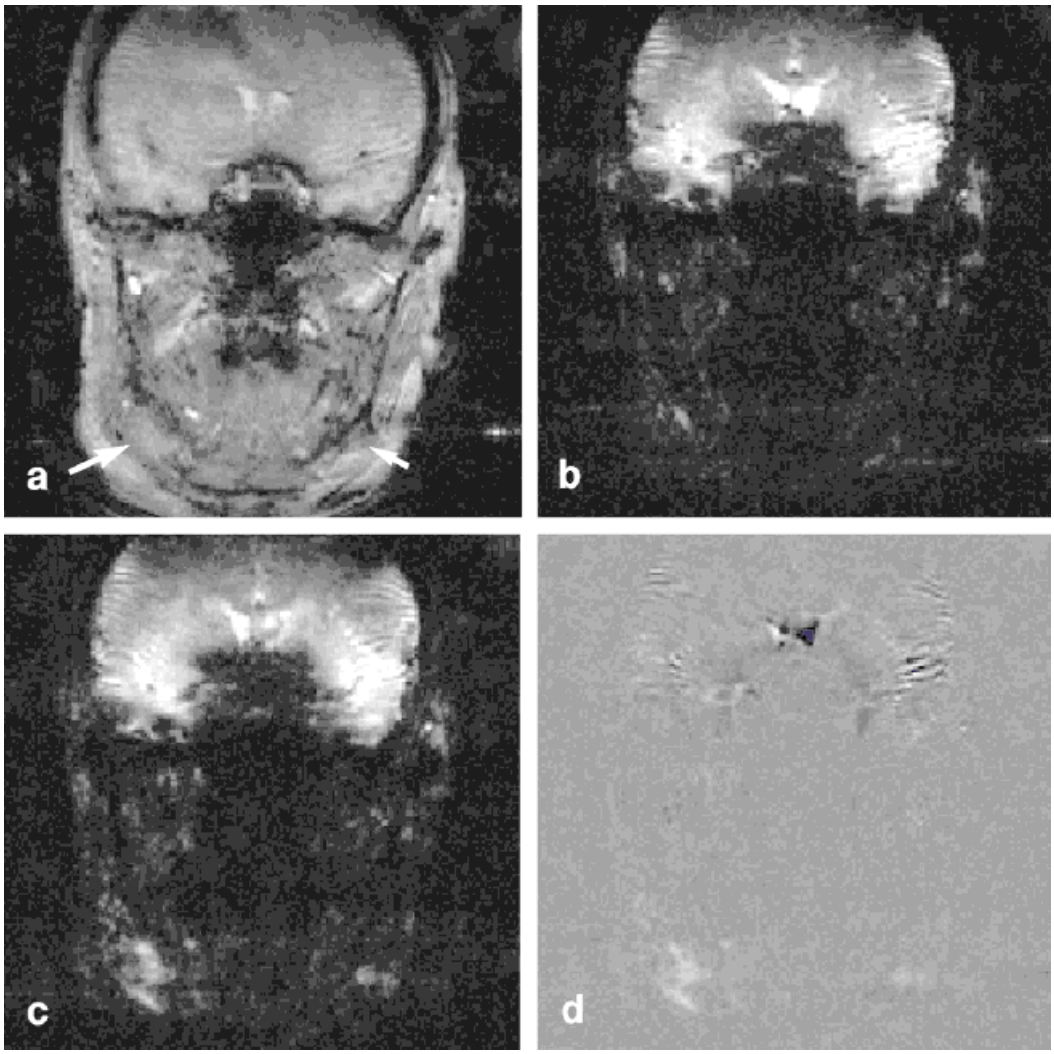

Figure 1. Coronal images of squamous carcinoma metastases from patient * in Table 1a. **a:** T_1-weighted scout image. **b:** T_2^*-weighted mean air image. **c:** T_2^*-weighted mean carbogen image. **d:** Subtraction image (c – b). The arrows on image a indicate the metastatic deposits: the larger arrow indicates the main metastasis, and the smaller arrow the previously unknown metastasis.

Brain

The response of the brain to carbogen was assessable in 13 patients with head and neck tumors. Eleven patients had significant brain enhancement (mean enhancement 8.0 ± 1.1%) and two had none (Table 1a).

Normal Prostate Glands

During the study of bladder carcinoma in men, it was observed that the prostate gland also enhanced, despite not being involved with the tumor. A volunteer study was carried out to see if the magnitude of the normal change in the prostate gland was comparable with tumor change.

Measurements on the normal prostates of 10 young (median age 33 years, range 27–39 years) and three older men (two aged 64 years and one 72 years) were carried out with carbogen breathing. Four of the volunteers were completely normal, and nine were patients with tumors in tissues other than the prostate (one transitional carcinoma of the bladder and eight testicular teratomas). The nine successful results are given in Table 2 and four technical failures are given in Table 1b. Figure 3 shows scout, subtraction, and air/carbogen BOLD images for the normal volunteer indicated by * in Table 2. Technically, the measurements were difficult due to the presence of air in the rectum causing susceptibility artifacts. These obscured any carbogen-induced signal change in four measurements. In addition, two of the volunteers were mildly claustrophobic and moved.

There was no significant MR signal intensity change in four measurements, and a significant change in five (mean 11.4%, range 8.4–14.0%). There was no apparent correlation with age.

DISCUSSION

The carbogen mixture generally had a significant effect on the respiration rate, but did not increase the pulse rate in most patients. The magnitude of any carbogen response detectable on the MR images did

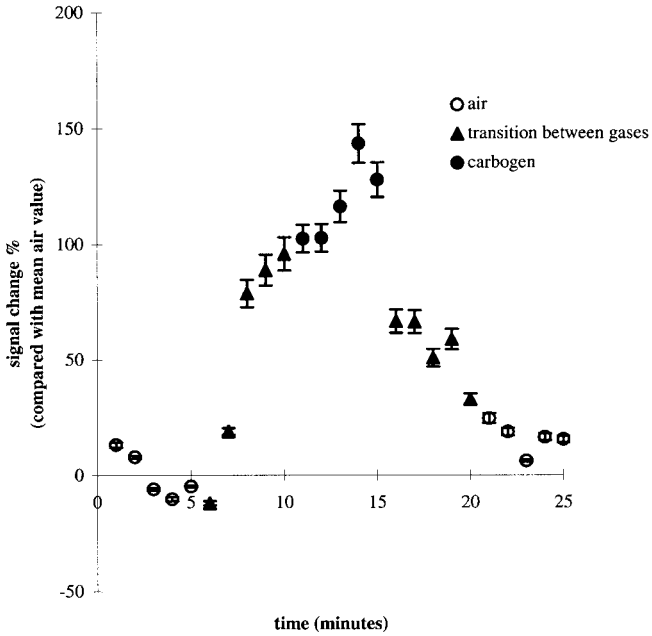

Figure 2. The signal changes (including transition values) corresponding to an ROI over the main tumor in patient * in Table 1a. Tumor position is shown by the large arrow in Figure 1a. The patient moved during the first five scans before settling; those data are omitted from this graph for clarity. Error bars denote ± 2 standard errors about the mean signal intensity within the ROI.

not correlate with either the pulse rate or respiration rate changes.

Carbogen is known to be a potent vasodilator (24) which leads to two effects that can alter the signal intensities observed on T_2^*-weighted MR images. These are an increase in the flow of magnetically unsaturated spins into an imaging slice (increased perfusion) or an increase in the O_2 saturation of blood with a relative increase in the oxy:deoxyhemoglobin ratio (6,22). Computerized Eppendorf oxygen probe measurements and laser-based Doppler blood flowmetry enable these two contrast mechanisms to be disentangled. Human (11–13,25) and animal (26) Eppendorf measurements during carbogen breathing show significant changes in tissue oxygenation. Laser Doppler flowmetry, however, shows little change in macroscopic flow patterns (27,28). These results suggest that the most important effect shown in the T_2^*-weighted MR images of tumors is likely to be the signal change due to blood oxygen saturation changes. In our MR sequence, the relatively long TR makes the sequence both oxygen- and flow-sensitive, in order to detect changes in both oxygenation and blood flow to the tumors induced by the carbogen. An SSFP image at long TR is similar to a conventional spoiled GE, while having slightly better flow sensitivity and SNR.

We observed increases in signal intensity in 20 of 36 patients on T_2^*-weighted MR images in responsive tissues over the baseline air-breathing intensities. It is also possible that carbogen-induced perfusion changes (27,28) within tumors might account for some increase in signal in addition to the altered hemoglobin oxygenation. Sixteen tumors did not show a significant signal change in response to carbogen. In cases of extreme vasoconstriction or vessel occlusion, in the absence of vessels, or the presence of a high proportion of immature vessels, vasodilation may not occur. In these circumstances, no signal change would be observed. Well perfused, highly oxic tumors also would show no significant signal change.

Perfusion and oxygenation levels within human tumors are known to be heterogeneous (11–13,25). Our results are consistent with this observation. Most tumors that showed some response to the carbogen did not respond equally throughout the slice examined. The mean signal changes given in the tables do not show the heterogeneous response, which can be seen clearly in Figure 1.

On carbogen breathing, two tumors (breast adenocarcinoma and the antrum cystic carcinoma (both marked with + in Table 1a) showed significant areas of reduced T_2^*-weighted signal adjacent to areas of increased signal, which suggests that a "vascular steal" phenomenon may have occurred (29), although the overall change in the breast tumor was a signal intensity increase, and in the antrum tumor a signal intensity decrease.

The very well perfused gray matter within normal brain is known to dilate in the presence of carbon dioxide (21). This would tend to increase the blood volume and flow, and therefore the MR signal intensity in T_2^*-weighted images. In this study we observed significant signal increases in 10 of 12 normal brains, regardless of the tumor response. The 8.0% mean increase seen with our 5% CO_2:95% O_2 mixture is comparable with the 6.81% observed by Rostrup et al (21) with a 5% CO_2:air mixture at a similar field strength, with the additional enhancement attributable to our use of oxygen instead of air. Of the two patients who did not show a significant increase in brain signal, one showed no tumor increase. Improper mask fitting may have been a contributing factor in this case (30).

Our prostate study shows that susceptibility artifacts caused by air and feces in the rectum are a significant limiting factor. These artifacts can be minimized by asking patients to evacuate before the MRI examination. The ability of normal prostate tissue to enhance should not come as a surprise. It is well known that normal prostate tissues produce high levels of endoge-

Table 2
Successful Prostate Measurements

Age in years	Mean signal change (%)	*P*
64+	8.4 ± 3.7	$P = 0.024$
64+	11.7 ± 0.4	$P < 0.001$
36+	13.4 ± 6.7	$P < 0.001$
39+,*	14.0 ± 12.0	$P = 0.02$
31+	9.5 ± 7.3	$P = 0.009$
72+	NSR	
33+	NSR	
35§	NSR	
33§	NSR	

+Volunteers with tumours outside the prostate.
*Volunteer shown in Figure 3.
§ = Volunteers with no tumor.

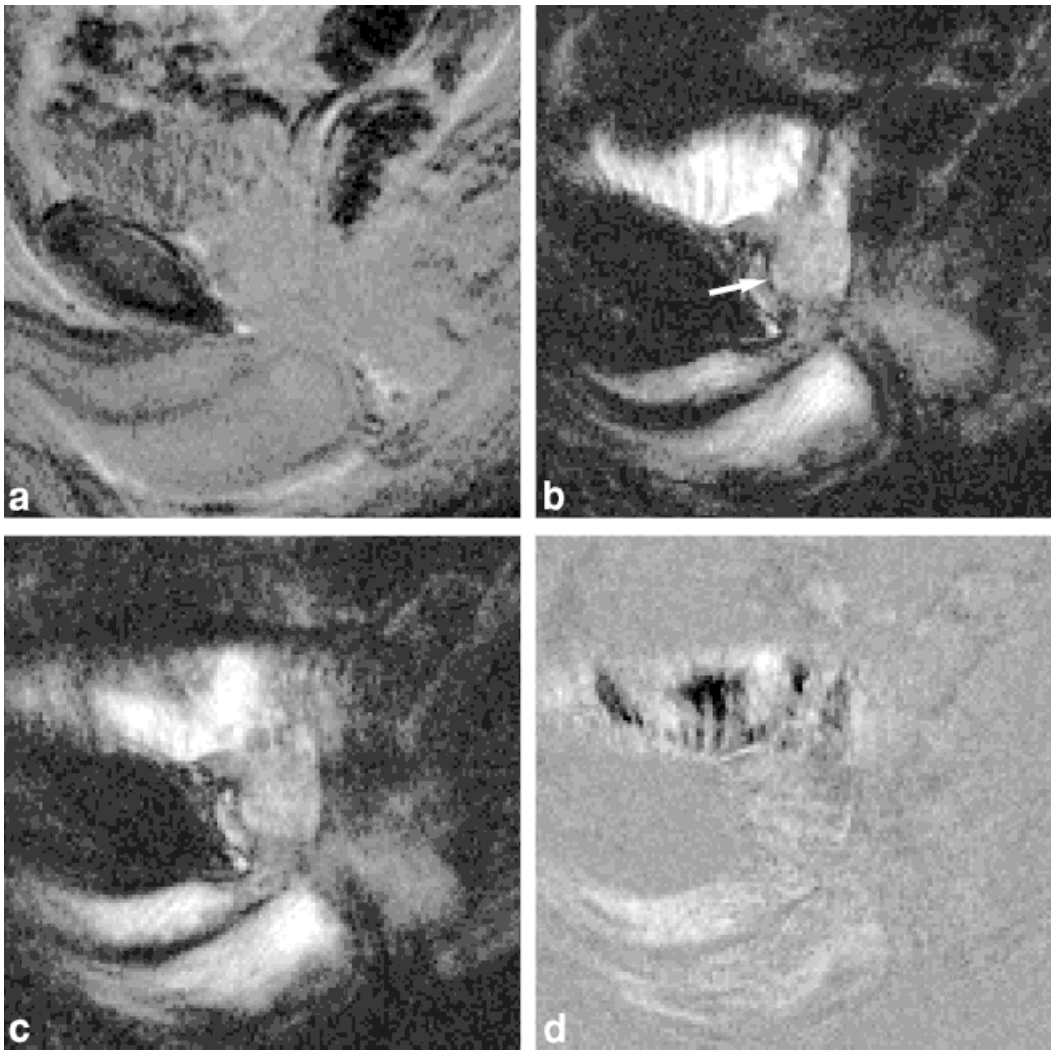

Figure 3. Sagittal images of a normal prostate (arrow on image **b**) from volunteer * in Table 2. The bladder is the bright region above the prostate on the T_2^*-weighted images. **a:** T_1-weighted scout image. **b:** T_2^*-weighted mean air image. **c:** T_2^*-weighted mean carbogen image. **d:** Subtraction image (c – b).

nous vascular endothelial growth factor (VEGF), a potent stimulus of angiogenesis. The role of prostatic VEGF has not been completely defined, but is thought to be essential for the activation of spermatozoa (31,32). The presence of enhancement within prostate tissues also suggests that this technique may not be suitable for the study of patients with prostatic cancer, particularly at the spatial resolution of the current study. Recently, using a body array coil with a Siemens 1.5T Symphony MR scanner (Erlangen, Germany) we were successful in obtaining images of the prostate at higher resolutions, which showed good correlation between the site of known tumors and T_2^*-weighted signal. There was no significant difference between the magnitude of prostate enhancement of normal volunteers and those who had an underlying malignancy.

CONCLUSIONS

It may be concluded that T_2^*-weighted MRI provides a noninvasive method of assessing the response of individual tumors to carbogen, and may help identify those patients who are likely to benefit from radiosensitization with carbogen. The methods described are technically challenging for patients because of respiratory distress caused by inhalation of the carbogen mixture. Gases with lower ratios of CO_2:O_2 may be more suitable for clinical use.

ACKNOWLEDGMENTS

We thank the Department of Anaesthesia at Mount Vernon Hospital and BOC Limited (Guildford, UK) for help and advice.

REFERENCES

1. Kwong KK, Belliveau JW, Chesler DA, et al. Dynamic magnetic resonance imaging of human brain activity during primary sensory stimulation. Proc Natl Acad Sci USA 1992;89:5675–5679.
2. Taylor NJ, Griffiths JR, Howe FA, et al. Carbogen-induced oxygenation and blood flow changes within human tumours, monitored by gradient echo magnetic resonance imaging. In: Proceedings of the 4th Annual Meeting of ISMRM, New York, 1996. p 1313.

3. Griffiths JR, Taylor NJ, Howe FA, et al. The response of human tumours to carbogen breathing, monitored by gradient-recalled echo magnetic resonance imaging. Int J Radiat Oncol Biol Phys 1997;39:697–701.
4. Gray LH, Conger AD, Ebert M, Hornsey S, Scott OCA. The concentration of oxygen dissolved in tissues at the time of irradiation as a factor in radiotherapy. Brit J Radiol 1953;26:638–648.
5. Saunders M, Dische S. Clinical results of hypoxic cell radiosensitisation from hyperbaric oxygen to accelerated radiotherapy, carbogen and nicotinamide. Br J Cancer 1996:74 (Suppl. XXVII) S271–S278.
6. Grau C, Horsman MR, Overgaard J. Improving the radiation response in a C3H mouse mammary carcinoma by normobaric oxygen or carbogen breathing. Int J Radiat Oncol Biol Phys 1992;22: 415–419.
7. Dische S. Hyperbaric oxygen. The Medical Research Council trials and their clinical significance. Br J Radiol 1978;51:888–894.
8. Dische S. What have we learnt from the work with hyperbaric oxygen? Radiother Oncol 1991; Suppl. 20:71–74.
9. Kruuv JA, Inch WR, McCredie JA. Blood flow and oxygenation of tumours in mice: I. Effects of breathing gases containing carbon dioxide at atmospheric pressure. Cancer 1967;20:51–59.
10. Rojas A. ARCON: accelerated radiotherapy with carbogen and nicotinamide. Brit J Radiol 1992; suppl. 24:174–178.
11. Falk SJ, Ward R, Bleehen NM. The influence of carbogen breathing on tumour tissue oxygenation in man evaluated by computerised pO_2 histography. Br J Cancer 1992;66:919–924.
12. Martin L, Lartigau E, Weeger P, et al. Changes in the oxygenation of head and neck tumours during carbogen breathing. Radiother Oncol 1993;27:123–130.
13. Powell MEB, Collingridge DR, Saunders MI, Hoskin PJ, Hill SA, Chaplin DJ. Improvement in human tumour oxygenation with carbogen of varying CO_2 concentrations. Radiother Oncol 1999;50: 167–171.
14. Overgaard J. Modification of hypoxia—from Gottwald Schwarz to nicotinamide. Have we learned the lesson? In: Progress in radiooncology. V. Bologna: Monduzzi Editore; 1995. p 469–475.
15. Ogawa S, Lee T-M, Nayak AS, Glynn P. Oxygenation-sensitive contrast in magnetic resonance image of rodent brain at high magnetic fields. Magn Reson Med 1990;14:68–78.
16. Kennan RP, Scanley BE, Gore JC. Physiologic basis for BOLD MR signal changes due to hypoxia/hyperoxia: separation of blood volume and magnetic susceptibility effects. Magn Reson Med 1997; 37:953–956.
17. Zhong J, Kennan RP, Fulbright RK, Gore JC. Quantification of intravascular and extravascular contributions to BOLD effects induced by alteration in oxygenation or intravascular contrast agents. Magn Reson Med 1998;40:526–536.
18. Robinson SP, Howe FA, Griffiths JR. Noninvasive monitoring of carbogen-induced changes in tumor blood flow and oxygenation by functional magnetic resonance imaging. Int J Radiat Oncol Biol Phys 1995;33:855–859.
19. Howe FA, Robinson SP, Griffiths JR. Discrimination of blood flow and oxygenation changes in rat tumors in response to carbogen breathing. In: Proceedings of SMR, 1995. p 64.
20. Howe FA, Robinson SP, Griffiths JR. Modification of tumour perfusion and oxygenation monitored by gradient-recalled echo MRI and ^{31}P MRS. NMR Biomed 1996;9:208.
21. Rostrup E, Larsson HBW, Toft PB, et al. Functional MRI of CO_2 induced increase in cerebral perfusion. NMR Biomed 1994;7:29–34.
22. Baddeley H, Brodrick P, Taylor NJ, et al. Gas exchange parameters during breathing of 2%, 3.5% and 5% carbogen gas mixtures in radiotherapy patients. Brit J Radiol 2000;73:1100–1104.
23. Siemann DW, Hill RP, Bush RS. The importance of pre-irradiation breathing times of oxygen and carbogen (95% O_2; 5% CO_2) on the *in vivo* radiation response of a murine sarcoma. Int J Radiat Oncol Biol Phys 1977;2:903–911.
24. Hill SA, Collingridge DR, Vojnovic B, Chaplin DJ. Tumour radiosensitisation by high-oxygen-content gases: influence of the carbon dioxide content of the inspired gas on pO_2, microcirculatory function and radiosensitivity. Int J Radiat Oncol Biol Phys 1998;40: 943–951.
25. Vaupel P, Schlenger K, Knoop C, Höckel M. Oxygenation of human tumors: evaluation of tissue oxygen distribution in breast cancers by computerised O_2 measurements. Cancer Res 1991;51:3316–3322.
26. Kallinowski F, Zander R, Höckel M, Vaupel P. Tumor tissue oxygenation as evaluated by computerised-pO_2-histography. Int J Radiat Oncol Biol Phys 1990;19:953–961.
27. Chaplin DJ, Hill SA. Temporal heterogeneity in microregional erythrocyte flux in experimental solid tumours. Brit J Cancer 1995; 71:1210–1213.
28. Powell MEB, Hill SA, Saunders MI, Hoskin PJ, Chaplin DJ. The effect of carbogen breathing on tumour microregional blood flow in humans. Radiother Oncol 1996;41:225–231.
29. Karczmar GS, Yu C, Kuperman V, Lewis MZ, River JN, Lubich L, Halpern H. Inhalation of 100% oxygen may decrease oxygenation in some tumor regions: magnetic resonance evidence for an intratumoral steal effect. In: Proceedings of SMR, 1995: p 1678.
30. Hoskin PJ, Abdelath O, Phillips H, Gilligan S, Saunders M, Broderick P, Baddeley H. Inspired and expired gas concentrations in man during carbogen breathing. Radiother Oncol 1999;51:175–177.
31. Ferrer FA, Miller LJ, Andrawis RI, Kurtzman SH, Albertsen PC, Laudone VP, Kreutzer DL. Angiogenesis and prostate cancer: in vivo and in vitro expression of angiogenesis factors by prostate cancer cells. Urology 1998;51:161–167.
32. Jackson MW, Bentel JM, Tilley WD. Vascular endothelial growth factor (VEGF) expression in prostate cancer and benign prostatic hyperplasia [see comments]. J Urol 1997;157:2323–2328.